Possible Feedback Path for Low-Frequency Atmospheric Oscillations

X. H. GAO AND J. L. STANFORD

Physics Department, Iowa State University, Ames, Iowa

(Manuscript received 30 December 1986, in final form 5 October 1987)

ABSTRACT

Equatorial low-frequency oscillations with periods of 1–2 months are being intensively studied by many investigators. A strong equatorial "dipole" pattern is observed in which atmospheric variables such as temperature, wind, and pressure are out of phase between the Indian Ocean–Indonesia region and the western Pacific. While it is generally thought that the oscillations make a complete circuit around the earth from their excitation region in the equatorial Indian Ocean–western Pacific, the signal is more difficult to observe over the South America–Atlantic–Africa sector. Using analyses of four years of satellite-derived microwave radiance data, evidence is presented here for the possibility of a feedback route in the Southern Hemisphere. The observed propagation path extends from the central equatorial Pacific across lower South America and heads equatorward after passing south of Africa. The response route finally reenters the equatorial Indian Ocean with correct phase to enhance the primary equatorial dipole structure. The Southern Hemisphere propagation path migrates northward in April–September and southward in October–March. The largest correlation with the equatorial dateline region occurs at the turning point of the feedback route, in the South Atlantic. This propagation path appears to constitute a feedback mechanism which could aid in stabilizing the low frequency oscillations through positive feedback.

The correlations are shown to be statistically significant by several methods, including Monte Carlo simulations.

1. Introduction

Low-frequency atmospheric oscillations (LFO) with periods of order 1–2 months have been studied in the tropics for many years by various investigators. Although many aspects of the oscillations are well known from these observational studies and modeling simulations, the mechanism causing the oscillation is not yet fully understood. Investigating 5–10 years of data from tropical stations, Madden and Julian (1971, 1972) discovered the 40–50 day oscillation. They raised the question of why this oscillation has a preferred time scale, and conjectured that the phenomenon is probably associated with a feedback mechanism, such as sea-surface temperatures and atmospheric circulation or evaporation and precipitation.

A possible mechanism is that convective heating over the Indian and western Pacific Oceans generates a wave which travels eastward around the earth and returns with the correct phase for positive feedback to the convection over the Indian Ocean.

The eastward propagating LFO feature over the equatorial Indian and western Pacific Oceans has been confirmed by a number of observational studies (e.g., Murakami et al. 1986; Murakami et al. 1984; Lau and Chan 1985; Weickmann 1983); however, the expected oscillation signal has proven difficult to identify at all longitudes around the Equator. The summer of 1979, with anomalously strong LFO and monsoon activities, had LFO signals in the velocity potential (divergence wind) which made a complete circuit around the globe (Krishnamurti et al. 1985; Lorenc 1984). But the observed signal over tropical South America–Atlantic Ocean–Africa was in fact weak. Furthermore, after analyzing eight years of OLR (outgoing longwave radiation) data, Murakami et al. (1986) concluded that the phase propagation of low frequency oscillations is poorly organized over equatorial South America–Atlantic Ocean–Africa.

It appears that the LFO feature loses its energy, due to dissipation in the tropics, after traveling eastward away from the monsoon region and cannot usually make a complete circuit around the earth. The question can then be asked: are there other possible propagation routes around the world which, by positive feedback, might stabilize the low frequency oscillation?

Numerical models show that convective heating in the tropics can generate two different modes of disturbances: Kelvin modes which propagate eastwards along and are confined to latitudes near the Equator, and Rossby modes which move to the extratropics along a great circle route and return to low latitudes (Lim and Chang 1983; Gill 1980; Garcia and Salby 1986). The equatorial modes apparently cannot usually complete the whole trip around the earth, due to damping and lack of reamplification. On the other hand, the Rossby modes may conceivably pass through the midlatitudes

Corresponding author address: Dr. John L. Stanford, Dept. of Physics, Iowa State University, 12 Physics Building, Ames, IA 50011.

where instability mechanisms may feed energy into the low frequency disturbances through non-linear interactions. If such reamplified disturbances turned back towards the tropics again, positive feedback could occur. In fact, this tropics–extratropics–tropics feedback has already been hinted at by both observational and theoretical studies. Analysis of the Indian summer monsoon revealed an interesting northward propagation of low frequency perturbations originating in the Southern Hemisphere near 15°S (Murakami et al 1984; Yasunari 1980). In addition, a number of authors have presented evidence for LFO in extratropical regions (e.g., Anderson and Rosen 1983; Krishnamurti and Gadgil 1985; Gao and Stanford 1987; Graves and Stanford 1987). Murakami and Nakazawa (1985) analyzed FGGE level IIIb data and showed from studies of the energetics of 45 day oscillations that there are two "bridges" (50°–150°E and 170°–70°W) through which the 45-day perturbations had interhemispheric interactions. It was also found that over the eastern equatorial south Pacific, east of South America and east of southern Africa, the 45-day oscillations received kinetic energy through nonlinear barotropic interactions with seasonal mean and short-period transient disturbances. In another study, Hendon and Hartmann (1985) examined the variability in a two-level nonlinear spherical atmosphere model with zonally symmetric forcing. Their results show that the energy of disturbances cascades from the scale of baroclinic instability towards larger spatial and temporal scales. Their model produces a large amount of low-frequency variance in subtropical and polar latitudes. These authors pointed out that substantial low-frequency variability would exist even without any direct forcing; the development of low-frequency disturbances can be expected as a result of nonlinear transfer of energy from the scale of baroclinic instability.

The purpose of the present paper is to present evidence for a possible extratropical propagation route which could help stabilize the low frequency oscillations through positive feedback. Four years of global satellite-derived microwave brightness temperature (T_b) are analyzed and the results imply a possible feedback route for 40–50 day oscillations. The propagation path is along an approximate great circle from the equatorial Indian Ocean to the central Pacific region, to the southeast Pacific, to the south Atlantic, across southern Africa, and returning to the equatorial Indian Ocean.

2. Data and analysis

In this study four years (from 1 April 1980 to 31 March 1984) of MSU4 (Microwave Sounder Unit, Channel 4) data have been analyzed for 40–50 day oscillations. The central frequency of the MSU4 channel is 57.95 GHz, and its weighting function peaks near 90 mb. The brightness temperatures obtained are approximately the 30–150 mb mean temperature, so that the measurements partly overlap the upper troposphere in the tropics where the high tropical tropopause usually is near 100 mb; outside the tropics, the data are representative of the lower stratosphere.

Nonoverlapping three day means are obtained from daily T_b 5° × 5° global grids produced by the British Meteorological Office. Space and time Fourier coefficients are obtained by Fast Fourier Transformation. Most of the results presented in this paper are based on these Fourier coefficients. Further data processing details are given in Gao and Stanford (1987).

A bandpass filter having a window in the frequency domain is used. The filter has 25 spectral points and half-amplitude periods of 41 and 49 days.

To avoid an instrumental "scan angle effect" which results in fallacious spectral peaks near zonal wavenumber 14 (Yu and Stanford 1984) and to enhance the signal-to-noise ratio for the large-scale disturbances of interest here, a spatial filter also has been used in which zonal mean and short-scale features (zonal wavenumbers higher than 10) are removed.

The correlations between band pass filtered time series are calculated in the frequency domain. The band pass filtered temperature time series is

$$T(r, t) = \sum_{\Delta\omega} [C_n(r) \cos\omega_n t + S_n(r) \sin\omega_n t]. \quad (1)$$

Here r is grid index (position of grid point), t is time, C_n and S_n are Fourier coefficients, n is Fourier frequency number, $\Delta\omega$ is the filter band, and $\omega_n = n \cdot 2\pi/(1464 \text{ day})$. The correlation between grid points r and q is

$$R(r, q) = \sum_t T(r, t)T(q, t)/\sigma_r\sigma_q = \frac{N}{2} \sum_{\Delta\omega} [C_n(r)C_n(q) + S_n(r)S_n(q)]/\sigma_r\sigma_q \quad (2)$$

with

$$\sigma_r^2 = \frac{N}{2} \sum_{\Delta\omega} [C_n(r)C_n(r) + S_n(r)S_n(r)].$$

The lag correlations are also calculated in the frequency domain. The Fourier coefficients of a lagged time series can be obtained by a rotation in the frequency domain. The data are interpolated for an extra period, equal to the lag, and then the lag correlations calculated in the frequency domain. The lag correlations obtained in this way do not differ significantly from ordinary lag correlations when the data record is much longer than the signal periods of interest. Further details of this technique are presented in a separate paper (Gao and Stanford 1988).

To investigate the seasonal influence on the 40–50 day oscillation features, the correlations and lag correlations are computed separately using band pass filtered data for summer and winter seasons. Here sum-

mer indicates 1 April to 30 September, and winter means 1 October to 31 March. The combination of band pass filter and summer (winter) projection provide a simple method for calculating correlations and lag correlations in the frequency domain. The main points of this method are: 1) the summer (winter) projection is the result of a projection operator acting on the time series, leading to improved efficiency in computing; 2) the projection operator in the frequency domain can be expanded in a series for which, when acting on a band pass filtered time series, only a few leading terms contribute to the correlation. Details of this computationally efficient method are given in Gao and Stanford (1988).

3. Results

a. One-point correlations maps

The main purpose of this paper is to investigate the extratropical 40–50 day disturbances which relate to the tropical low frequency oscillations. Many atmospheric phenomena exist in the middle latitudes and produce a rich spectrum of disturbances. To isolate LFO which are related to the tropical oscillations, we utilize one-point correlation maps with the reference point at the equator, 175°W. There are two reasons for choosing this reference point. First, here the 40–50 day signal is strong and has high signal-to-noise ratio in our data (Gao and Stanford 1987); second, this point is close to one of the two "bridges" for interhemispheric interaction (Murakami and Nakazawa 1985). Figures 1a–f are one-point correlation maps with 0, 5, 10, 15, 20 and 25 day lags, respectively. The data used to calculate the correlations are filtered 40–50 day brightness temperatures from MSU4 measurements (150–30 mb temperatures), filtered as described in section 2.

There are several interesting features in the correlation maps of Fig. 1.

1) The well-known "dipole" structure over the equatorial Indian and Pacific Oceans is clearly visible. These two regions with opposite phases are about 90° apart longitudinally and move eastwards with time (increasing lag) as an entity, consistent with earlier observations (for example, Lau and Chan 1985; Weickmann et al. 1985). Based on the lag correlation maps in Fig. 1, the phase speed of the dipole is approximately 4° per day, consistent with the 500 km day^{-1} value reported by Murakami et al. (1984) for zonal wind perturbations. The dipole feature in Fig. 1 has wave-two spatial scale, so that its 4° per day speed is consistent with the value of 8° per day reported by Murakami and Nakazawa (1985) for their 40–50 day zonal wavenumber one features.

2) Note that none of the lag correlation maps show significant correlation between equator, 175°W and equatorial longitudes stretching from South America across Africa. This result suggests that the 40–50 day features over those regions are significantly weakened or poorly related to that over the central Pacific Ocean, or both. A similar result is reported by Murakami et al. (1986) based on extended empirical orthogonal function analysis for eight years of OLR data.

3) In contrast to the lack of signal correlation over equatorial South America–Africa, significant correlations are observed along a path (denoted by dashed lines in Fig. 1) extending from the central equatorial Pacific into the Southern Hemisphere, crossing South America and under South Africa. The response route finally bends northward to reenter the equatorial Indian Ocean with correct phase to enhance the primary equatorial dipole structure discussed above. This propagation path thus appears to constitute a feedback route whereby the low frequency oscillations may be stabilized by positive feedback.

On the maps with 0, 5 and 20, 25 day lags (near zero and one-half period, respectively) this route is formed by a series of alternating high correlation and anti-correlation regions. On the maps with 10, 15 day (about one-fourth period) lags, the extratropical segments of this route are less well-defined, while the equatorial segments are still evident. These results confirm that in the tropical Indian Ocean–Indonesian–central Pacific region, the 40–50 day perturbations consist of large traveling wave components. Moreover, the results also indicate standing wave oscillations in the extratropics. It is interesting to note that the route leaves the tropics at one of the two interhemispheric "bridges" (in the eastern Pacific) reported by Murakami and Nakazawa (1985), and reenters the tropics at the other "bridge" they reported (in the Indian Ocean). Furthermore, the Southern Hemisphere propagation path in Fig. 1 traverses regions (tropical South Pacific at 90°–110°W, and subtropical western Indian Ocean) where Murakami and Nakazawa reported (their Fig. 10) that 45 day perturbations receive kinetic energy from the seasonal mean wind field and short period perturbations. Finally, it is worth noting that the features along the extratropical segment of the route are reminiscent of the wave trains produced by tropical heating in a number of modeling simulations.

4) Eastward and poleward of each "pole" of the dipole there are subtropical regions of high correlations, roughly symmetric about the equator. Each such region is anticorrelated with its respective tropical "pole" region. For example, in Fig. 1a there are negative correlations centered near 20°N, 110°W and 20°S, 100°W, as well as another pair near 15°N, 130°E and 25°S, 110°E. These suggest extratropical responses to tropical convective perturbation. The propagation path mentioned above in (3) passes over one of these subtropical response regions, the southeastern Pacific, with clearly organized features suggesting possible tropical–extratropical–tropical linkage. In addition, there are

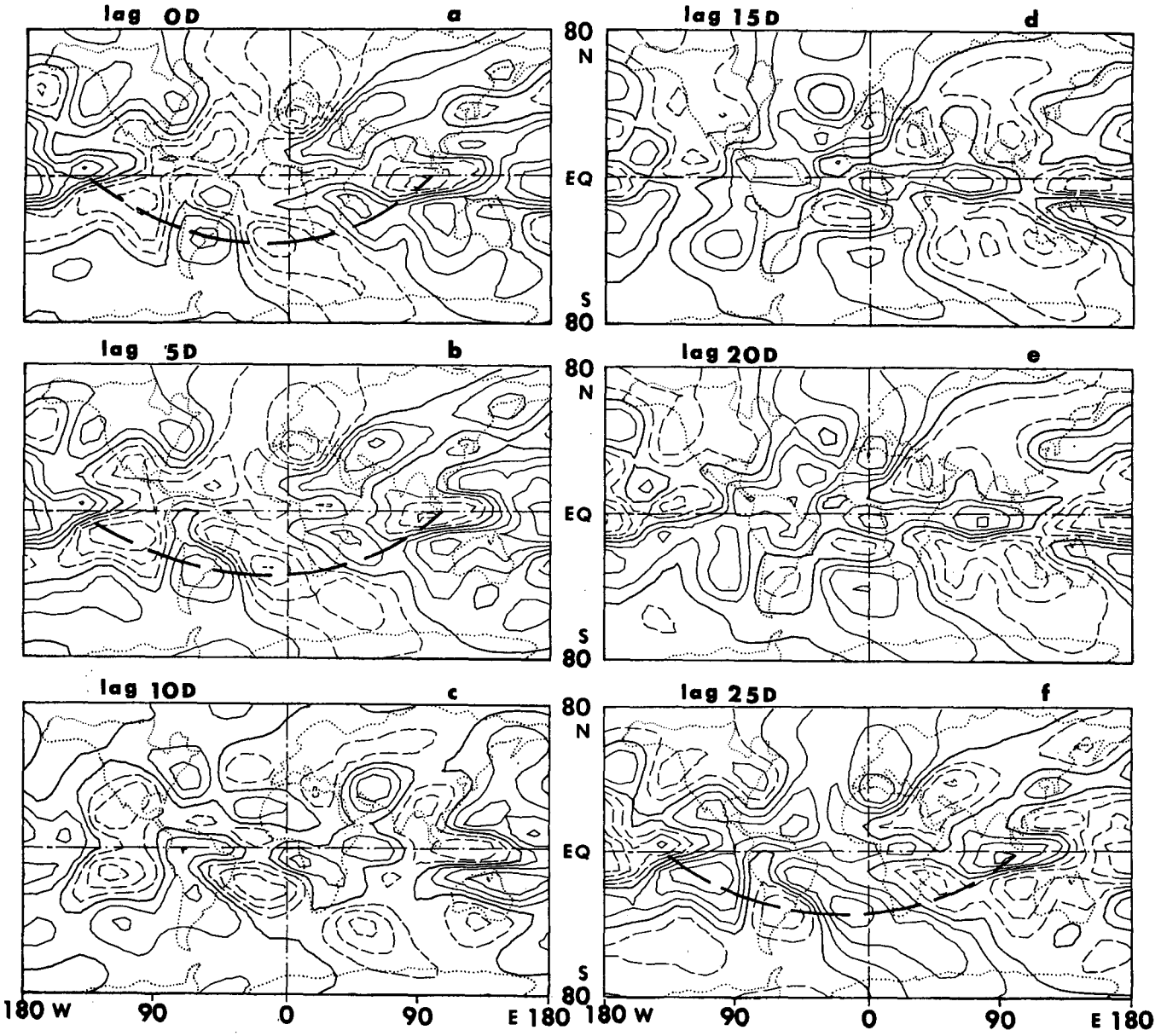

FIG. 1. All-season data, one-point correlation maps of 40–50 day filtered MSU4 brightness temperatures. Reference point: equator, 175°W. Contour level interval 0.2. Solid lines begin at $R = 0$, dashed lines indicate anticorrelations. Lag time (days) as indicated. Long dashed lines suggest possible propagation route. Data used: 1 April 1980–31 March 1984.

other subtropical and midlatitude regions exhibiting correlation with the central Pacific, such as the Northern Hemisphere (NH) patterns crossing over North Africa and down into the tropical Indian Ocean (Fig. 1). The NH response routes are not as well organized along clearly defined propagation tracks as in the SH.

5) The turning point of the LFO propagation path in the Southern Hemisphere over the southern Atlantic Ocean (near 35°S, 15°W), is strongly correlated with the equatorial central Pacific. The strongest anticorrelation point in the Northern Hemisphere is located near 35°N, 0°.

b. One-point correlation maps for summer and winter seasons

The correlation and lag correlation maps were also calculated using only NH summer (1 April–30 September) or NH winter (1 October–31 March) data for the four years. The results are shown in Fig. 2 (NH summer) and Fig. 3 (NH winter). The features found in the all season correlations (Fig. 1) are also generally found in the seasonal correlation maps. Comparison of Fig. 1 with Figs. 2 and 3 allows seasonal comparison of the LFO features:

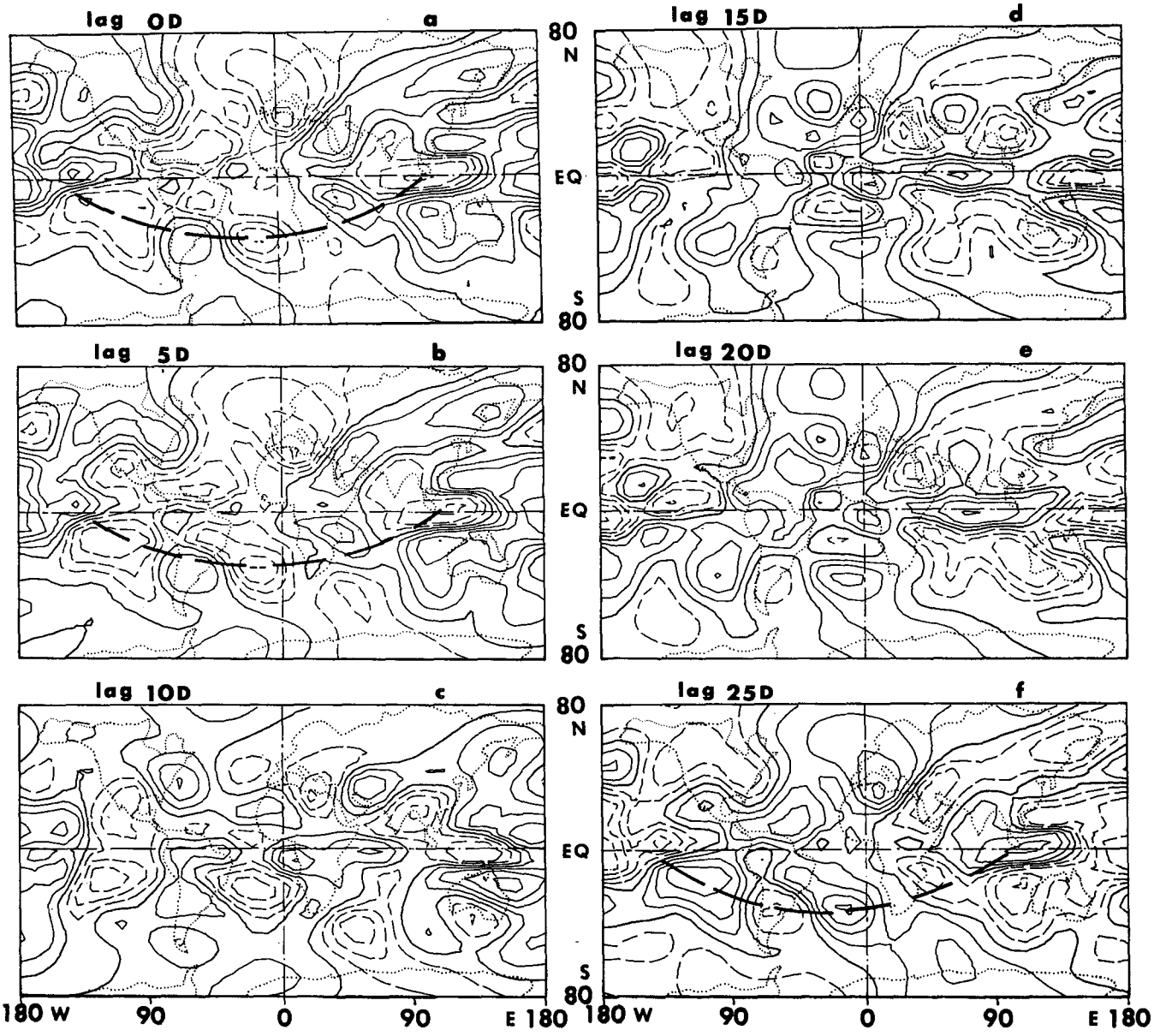

FIG. 2. As in Fig. 1 except for NH summer (1 April–30 September).

1) The direction and speed of propagation of the dipole structure over the tropical Indian and western Pacific Oceans are almost the same in both seasons. The small seasonal variation in eastward propagation speed requires further explanation, and will provide stringent tests for modeling.

2) The extratropical segments of the SH propagation path lies closer to the equator in the NH summer (SH winter) than in the NH winter (southern summer). The turning point of the propagation path is found at about 30°S in the SH winter and about 40°S in the SH summer. The turning point latitude may be related to the position of the tropospheric westerly jet and may be indicative of reflection of the low frequency waves due to the strong horizontal shear of the wind field in this region.

3) The correlation between the signals at the turning point and equatorial central Pacific is strongest in the NH summer (southern winter), in agreement with the model results of Garcia and Salby (1986). In the winter hemisphere the westerly winds are close to the equatorial convective heating source region, yielding favorable conditions for signal propagation from the tropical forcing region into the midlatitudes.

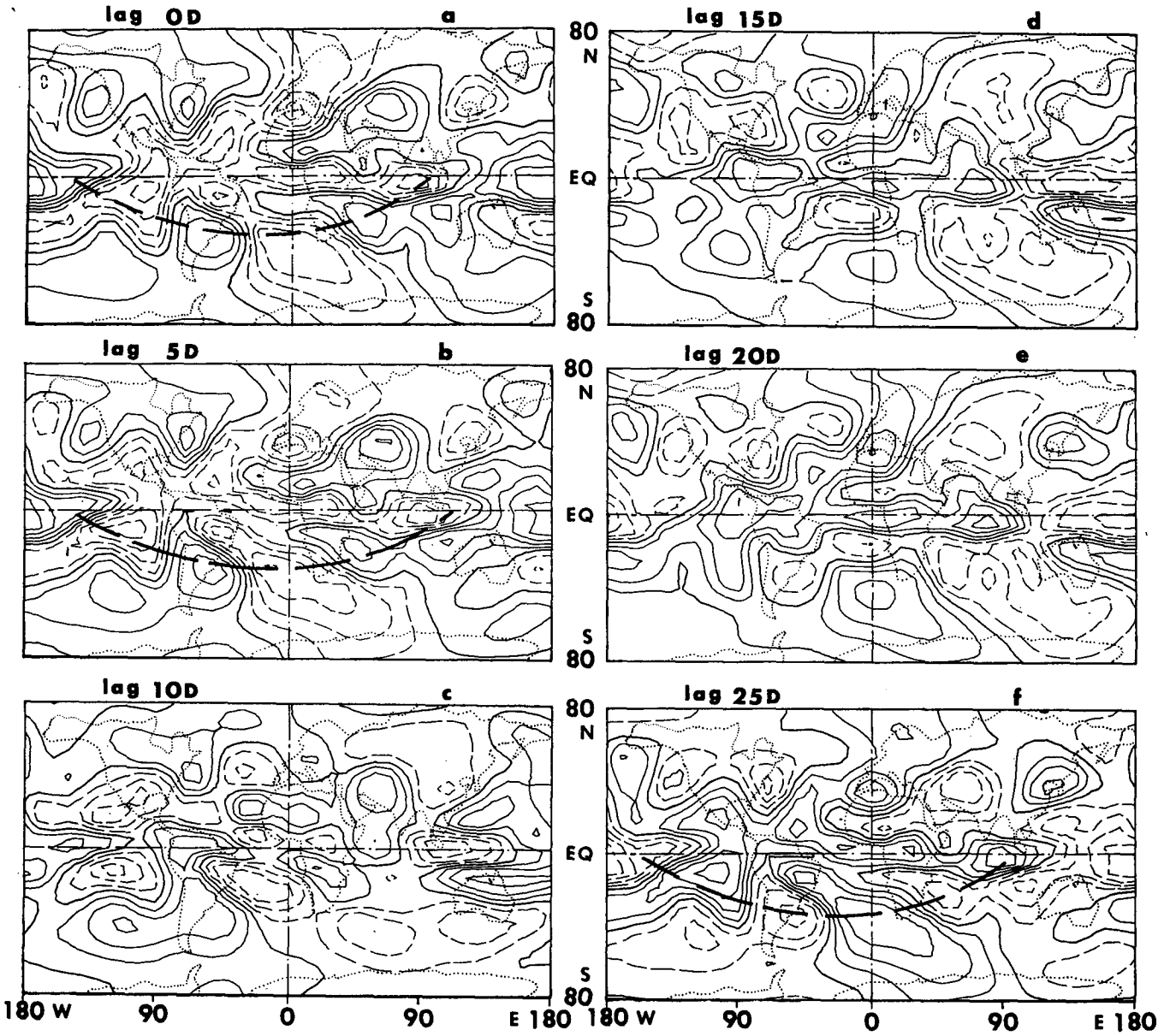

FIG. 3. As in Fig. 1 except for NH winter (1 October–31 March).

c. Confidence levels

There are three kinds of confidence levels being commonly used to determine statistical significance related to global correlation maps.

1) A 95% confidence level, R_L, is used to determine whether a previously selected region is significantly correlated with the map reference point. For example, to test whether the previously reported dipole structure over the equatorial western and central Pacific Ocean is observed in our one-point correlation map in Fig. 1, one may ask, "Is the equator, 95°E significantly anti-correlated with the reference point (equator, 175°W)?" Here a priori statistics should be used; for our case the confidence level is $R_L \approx 0.39$. Since the R value at the equator, 95°E is −0.70 (Fig. 1a), which exceeds R_L in magnitude, we conclude that the equator, 95°E point is significantly anticorrelated with the reference point.

2) The 95% confidence level, R_g, is used in a posteriori statistics. For a one point global correlation map, one may ask, "Is there a region anywhere on the globe having significant correlation with the reference point?" Because there are many grid points and thus more chance for a large correlation R to occur by random

processes, R_g must be set at a higher level than that in the a priori case (R_L) where only one (previously selected) grid point was examined; R_g may be determined by the method of Madden and Julian (1971). For our case $R_g \approx 0.68$. If anywhere on a correlation map there exists $R > R_g$, there is less than one chance in 20 that such a correlation would occur due to random fluctuations. As an example, in the correlation map of Fig. 1a, several high R regions are seen; in particular, $R \approx 0.80$ at 35°S, 15°W. Since this exceeds $R_g = 0.68$, the correlation between 35°S, 15°W and the reference point at the equator, 175°W can be considered statistically significant.

3) If correlations on a map exceed R_g, they can be taken as statistically significant. In many cases, however, the correlations may be less than R_g but still appear relatively large and cover sizeable map area. (It is important to note that if the number of spatial degrees of freedom are low, a map for which correlation is not significant may in fact exhibit large areas with similar correlation values, giving the appearance of correlation; this effect is related to the nonindependence of the grid points.) The statistical significance of such situations can be assessed by the technique suggested by Livezey and Chen (1983). Let $P(R)$ be the percentage of correlation map area with correlation $\geq R$. If $P(R)$ equals or exceeds a critical value dependent on R, say $P_c(R)$, it indicates that some map features are significantly correlated with the reference point.

Values of $P_c(R)$ were obtained from 200 Monte Carlo simulations appropriate to our analyses. The results suggest that areas of correlations higher than about $R = 0.35$ in Fig. 1 may be considered statistically correlated to the reference point, at the 95% confidence level.

4. Summary and discussion

- Near the tropopause, over the tropical Indian Ocean, western and central Pacific Ocean, 40–50 day disturbances in temperature show a dipole feature which propagates eastward with a speed of about 4° longitude per day.
- Possible propagation paths for the 40–50 day perturbations were found in the calculated correlation maps. In the Southern Hemisphere, the path is approximately along a great circle route from the equatorial central Pacific Ocean, through the extratropics along a southeastern Pacific–southern South America–south Atlantic Ocean–South Africa path; it returns to the equatorial Indian Ocean with correct phase to reinforce the dipole structure. Along the tropical segments of the route, the 40–50 day feature which is correlated with the central Pacific has large traveling components; along the extratropical segments the feature is characterized by standing waves. In the Northern Hemisphere, another path is possible, although less distinct. For example, a very strong correlation is observed over north Africa. Further studies are needed to clarify this feedback mechanism and its relative importance. In particular, calculations of the energetics of the 40–50 day disturbances in extratropical regions would be very helpful.
- The extratropical segments of the propagation path in the Southern Hemisphere lie closer to the equator in the SH winter than in the summer. The turning point is near 30°S for April–September, and near 40°S for October–March. The strongest anticorrelation to temperature disturbances over the central Pacific Ocean occur at the turning points, one lying in each hemisphere.

Acknowledgments. This paper is based upon work supported jointly by the National Science Foundation and the National Aeronautics and Space Administration under Grants ATM 8402901 and ATM 8603943. We especially appreciate helpful discussions on computing with Mr. L. R. Lait and statistics with Mr. C. E. Graves. We also thank Mrs. Wenbi Yu for helping with the graphs. Comments by two anonymous referees improved calculational details and clarity of the final manuscript.

REFERENCES

Anderson, J. R., and R. D. Rosen, 1983: The latitude-height structure of 40–50 day variations in atmospheric angular momentum. *J. Atmos. Sci.*, **40,** 1584–1591.

Gao, X. H., and J. L. Stanford, 1987: Low-frequency oscillations of the large-scale stratospheric temperature field. *J. Atmos. Sci.*, **44,** 1991–2000.

——, and ——, 1988: Improved efficiency for statistical calculations with globally-gridded filtered time series. *J. Climate,* in press.

Garcia, R. R., and M. Salby, 1986: Transient response to localized episodic heating in the tropics. Part II: Far field behavior. *J. Atmos. Sci.*, **44,** 499–530.

Gill, A. E., 1980: Some simple solutions for heat-induced tropical circulation. *Quart. J. Roy. Meteor. Soc.*, **106,** 447–462.

Graves, C. E., and J. L. Stanford, 1987: Low-frequency atmospheric oscillations over the southeastern Pacific. *J. Atmos. Sci.*, **44,** 260–264.

Hendon, H. H., and D. L. Hartmann, 1985: Variability in a nonlinear model of the atmosphere with zonally symmetric forcing. *J. Atmos. Sci.*, **42,** 2783–2797.

Krishnamurti, T. N., and S. Gadgil, 1985: On the structure of the 30 to 50 day mode over the globe during FGGE. *Tellus,* **37A,** 336–360.

——, P. K. Jayakumar, J. Sheng, N. Surgi and A. Kumar, 1985: Divergent circulations on the 30 to 50 day time scale. *J. Atmos. Sci.*, **42,** 364–375.

Lau, K. M., and P. H. Chan, 1985: Aspects of the 40–50 day oscillation during the northern winter as inferred from outgoing longwave radiation. *Mon. Wea. Rev.*, **113,** 1889–1909.

Lim, H., and C.-P. Chang, 1983: Dynamics of teleconnections and Walker circulations forced by equatorial heating. *J. Atmos. Sci.*, **40,** 1897–1915.

Livezey, R. E., and W. Y. Chen, 1983: Statistical field significance and its determination by Monte Carlo techniques. *Mon. Wea. Rev.*, **111,** 46–59.

Lorenc, A. C., 1984: The evolution of planetary scale 200 mb divergences during the FGGE year. *Quart. J. Roy. Meteor. Soc.*, **110,** 427–441.

Madden, R. A., and P. R. Julian, 1971: Detection of a 40–50 day oscillation in the zonal wind in the tropical Pacific. *J. Atmos. Sci.*, **28,** 702–708.

——, and ——, 1972: Description of global-scale circulation cells in the tropics with a 40–50 day period. *J. Atmos. Sci.*, **29,** 1109–1123.

Murakami, T., and T. Nakazawa, 1985: Tropical 45 day oscillations during the 1979 Northern Hemisphere summer. *J. Atmos. Sci.*, **42,** 1107–1122.

——, —— and J.-H. He, 1984: On the 40–50 day oscillations during the 1979 Northern Hemisphere summer. Part I: Phase propagation. *J. Meteor. Japan,* **62,** 440–468.

——, —— and ——, 1984: On the 40–50 day oscillations during the 1979 Northern Hemisphere summer. Part II: Heat and moisture budget. *J. Meteor. Japan,* **62,** 469–484.

——, L.-X. Chen, A. Xie and M. L. Shrestha, 1986: Eastward propagation of 30–60 day perturbations as revealed from outgoing longwave radiation data. *J. Atmos. Sci.*, **43,** 961–971.

Weickmann, K. M., 1983: Intraseasonal circulation and outgoing longwave radiation modes during Northern Hemisphere winter. *Mon. Wea. Rev.*, **111,** 1838–1858.

——, G. R. Lussky and J. E. Kutzbach, 1985: Intraseasonal (30–60 day) fluctuations of outgoing longwave radiation and 250 mb streamfunction during northern winter. *Mon. Wea. Rev.*, **113,** 941–961.

Yasunari, T., 1980: A quasi-stationary appearance of 30 to 40 day period in the cloudiness fluctuations during the summer monsoon over India. *J. Meteor. Soc. Japan,* **58,** 225–229.

Yu, W.-B., and J. L. Stanford, 1984: Stratospheric circulation in the southern summer/northern winter 1980–1981: Behavior of zonal waves 1–10. *J. Atmos. Sci.*, **41,** 2179–2188.